Journal of Luminescence 194 (2018) 565–568

Contents lists available at ScienceDirect

Journal of Luminescence

journal homepage: www.elsevier.com/locate/jlumin

Airy pattern on narrow photoluminescence spectrum of band to band recombination in CdTe:Te thin films

M. Becerril-Silva[a,*], M. Meléndez-Lira[b,1], J.R. Farias-Mancilla[b], O. Zelaya-Angel[b]

[a] Departmento de Física, Centro de Investigación y de Estudios Avanzados del IPN, P.O Box 14-740, México 07000, D.F., Mexico
[b] Departamento de Física y Matemáticas, Instituto de Ingeniería y Tecnología, Universidad Autónoma de Ciudad Juárez, Chihuahua, Mexico

ARTICLE INFO

Keywords:
Thin films
CdTe
Sputtering deposition
X-Ray, Optical characterization

ABSTRACT

Semiconductor CdTe:Te films were deposited by means of rf sputtering on glass substrates. The excess of Te gave place to a high number of Cd-vacancies (V_{Cd}) producing p-type CdTe films. The density of carriers produced a high strength surface electric field which allowed obtain the bandgap value employing modulated transmittance spectroscopy. The obtained bandgap value of 1.40 ± 0.01 eV was confirmed by absorption spectroscopy measures. The density of holes is so high that bandgap renormalization is observed. Photoluminescence (PL) measurements were carried out with the down-converted 883.2 nm (1.403 eV) line of the 441.6 nm wavelength of a He-Cd laser. This energy allows to produce a resonant excitation of the CdTe:Te films, in such a way that electrons from the conduction band (CB) can be just excited to the valence band (VB). The resonant excitation produced a PL spectrum of band to band electron-hole recombination showing discrete energy emissions that follow the pattern of oscillations corresponding to the Airy model for a quantum triangular potential well. The average width of signals of the higher energy oscillations is 12 ± 3 μeV and separation between energy levels is of the order of 12 ± 3 μeV.

1. Introduction

The high absorption coefficient and optical bandgap value of the semiconductor CdTe had kept alive the interest on this material for many years. Even when recent technological advances had allowed obtain commercial CdTe based solar cells with increased efficiency and lab cells with a record value of 21% it is still far from the theoretical limit established by the detailed balance approximation [1]. The efficiency improvement in CdTe based solar cells had detonated an increasing demand for it then it is necessary to develop alternatives to the slow traditional purification processes used nowadays [2]. Beside its application in the production of solar cells, CdTe is used in the fabrication of radiation detectors for astrophysical and medical applications [3] and high resolution imaging devices [4], among others. For these optical applications it is important to understand the reflection, absorption, and transmission processes of the light along with the photon emissions produced under excitation by means of light, heat, electric field, etc. In particular to improve the efficiency of CdTe based solar cells it is of paramount importance to understand the diverse processes associated with hole carriers [5]. In the past our group has characterized diverse aspects of the photoluminescence (PL) spectrum of CdTe films such as multiphonon emissions [6], the influence of Cadmium vacancies on it [7], the dependence of the energy bandgap on temperature [8], and more recently, the donor–acceptor pair effects on it [9]. Now, we are reporting the sharp photoluminescence (PL) of a p-type CdTe:Te polycrystalline film with a bandgap value (E_g) of 1.40 ± 0.01 eV, which occurs when the excitation source is the 883.2 nm line (1.404 eV) obtained by down conversion of the 441.6 nm light of a He-Cd laser. The similar values between the energies of the bandgap and PL excitation line produces a resonant excitation in the CdTe films. The CdTe films were deposited by the RF sputtering technique employing an additional source of Te in order to obtain samples with a high content of Te. The surface states associated with the presence of cadmium vacancies produced an approximated triangular well with an electric field normal to the surface. It is worth to mention that the lower band gap value, as compared with that of a CdTe single crystal, is due to the high density of carriers associated to the Te content. The CdTe films were characterized by X-ray diffraction, X-Ray fluorescence spectroscopy and room temperature absorption, Raman, modulated transmission and PL spectroscopies. The hole density was obtained from Hall effect measurements. The band to band PL emission is accompanied at lower and higher energies than E_g by oscillations of

* Corresponding author.
E-mail address: becerril@fis.cinvestav.mx (M. Becerril-Silva).
[1] On sabbatical in UACJ-Chihuahua.

http://dx.doi.org/10.1016/j.jlumin.2017.09.011
Received 29 May 2017; Received in revised form 25 August 2017; Accepted 5 September 2017
Available online 06 September 2017
0022-2313/ © 2017 Elsevier B.V. All rights reserved.

intensity which follow an Airy pattern characteristic of quantum confinement in a triangular potential well.

2. Experimental

The Te rich CdTe sample was grown on a 7059 Corning glass substrate at room temperature (RT) using a balanced magnetron rf 13.5 MHz sputtering system with a water-cooled cathode. The system is monitored employing ion and pirani gauges. A pressure base of 10^{-6} Torr was attained prior to film deposition by employing a diffusion pump backed with a mechanical pump. The working plasma was produced using 10 mTorr of UHP Ar gas. The rf power utilized during the growth process was 30 W with a distance of 4 cm between the target and substrate. The glass substrates were cleaned by a standard technique using detergent and organic solvents. The extra Te atoms were introduced in the samples by co-sputtering from a single CdTe target on which a piece of elemental tellurium of purity of ~ 99.999% placed above. The cold pressed 1 in. diameter circular target was prepared using CdTe powder material with ~ 99.999% of purity from CERAC. The effective area of the metallic Te was approximately 2%, this figure is obtained taking in account the small erosion profile associated with the balanced magnetron sputtering process. The thickness of the CdTe film was 250 ± 10 nm as measured with a KLA TENCO P-15 profilometer. The Cd and Te contents in the films were measured by means of X-ray spectroscopy (EDS) using a Voyager II X-ray quantitative microanalysis in an1100/1110 EDX system from Noran Instruments, with an uncertainty of ± 1%. The determination of Cd and Te content was calibrated by employing CdTe polycrystal with a purity of 99.999% from CERAC. The sign and concentration of carriers were obtained through Hall Effect measurements, performed in a conventional apparatus from GMW magnet systems model 3472-50. The crystalline structure of the films was determined by x-ray diffraction patterns, measured with a diffractometer SIEMENS D5000, the system has an instrumental linewidth of 0.05° at 45° in the 2θ scale. The RT optical absorption spectra of the films were measured by using a UNICAM 8700 spectrophotometer. RT Raman spectroscopy was carried out employing a Jobin Yvon Labram micro Raman using the 632.8 nm HeNe laser line as excitation source. PL measurements were carried out at RT using as the excitation source the 441.6 nm (2.808 eV) line of an Omnichrome 2056 He-Cd laser with 35 mW of power. The 441.6 nm line was down-converted to 883.2 nm (1.404 eV) by means of a BBO filter. PL emission was analyzed using a 0.5 m Jovin-Ivon double spectrograph, endowed with a resolution better than 0.05 nm, and detected using a Ag–Cs–O Hamamatsu photomultiplier, with a spectral response in the range 400–1200 nm using standard lock-in technique. The modulated laser light was irradiated onto the sample by a spot radius of 1 mm. The fundamental band gap energy of the CdTe:Te layers was determined by RT modulated transmittance spectroscopy (MTS) employing a standard experimental setup, with modulation light provided by the 632.8 nm wavelength of a He-Ne laser. The chopped laser light was irradiated onto the sample by a spot radius of 1 mm. A 200 W tungsten lamp was dispersed by employing a 20-cm monochromator and used as the probe-light. The transmitted-probe light from the sample was detected by a Si detector, and the signal from the detector was fed to a lock-in amplifier.

3. Results and discussions

CdTe is a material that easily gets self-compensated and generally it is obtained with a slightly p-type conductivity. When it is grown as a single crystal p-type doping levels associated with Te are relatively low; it is reported a merely 2×10^{16} cm^{-3} value [10]. Higher contents of Te can be attained with deposition processes far from equilibrium such as rf sputtering. Usually as grown CdTe films deposited by rf sputtering from high purity CdTe targets result Te-rich. In order to obtain stoichiometric CdTe films, elemental Cd should be added to the target [11]. In the present case an excess of elemental Te was added to the target to reach a Te rich composition of 53 ± 1 at%. The CdTe with excess of Te is characterized to behave as p-type semiconductor mostly due to the Cd vacancies formation and interstitial Te [12]. The holes density calculated from Hall Effect measurements was $5.0 \pm 0.2 \times 10^{18}$ cm^{-3}. Fig. 1 displays the X-ray diffraction pattern of the sample studied where a polycrystalline cubic-zincblende structure is mainly displayed plus some hexagonal-wurtzite CdTe and hexagonal Te inclusions. From the width of peaks for low 2θ values in the diffractogram and using the Debye-Scherrer formula an average diameter of 18 ± 2 nm for the grains was calculated. The Bohr radius of CdTe is 7.3 nm, this means that this study lies in the intermediate regime of quantum confinement. The Raman spectrum of the CdTe:Te sample is shown in Fig. 2, clearly signals from CdTe and Te modes are present. The higher intensity of Te modes with respect to those of CdTe is consequence of the very large cross section of Te [13]. The existence of Te rich CdTe is in this way confirmed through these three different techniques. The high doping level due to the Te content is reflected through the presence of a surface electric field easily modulated by the generation of electron-hole pairs associated with the modulated transmission spectroscopy [14]. The bandgap energy (E_g) was calculated from modulated transmission spectroscopy measurements (MTS) by the fitting to the Aspnes model employing a tridimensional critical point [15]. The experimental MT spectrum along with the theoretical fitting is shown in Fig. 3. This value

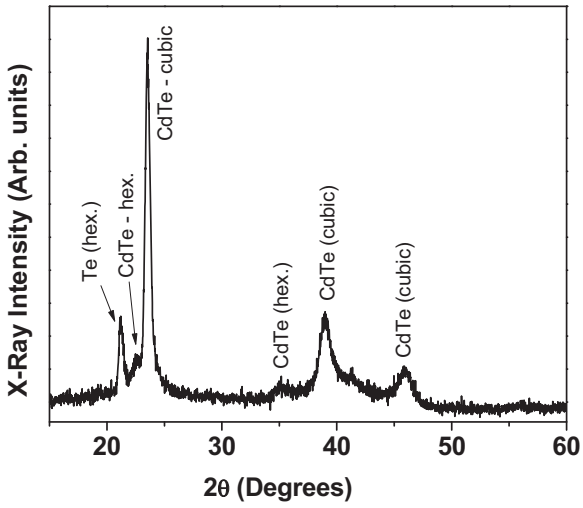

Fig. 1. X-ray diffraction pattern of a CdTe:Te sample where the film has essentially the cubic-zincblende structure. Inclusions of hexagonal-wurtzite CdTe and hexagonal Te are also observed in the sample.

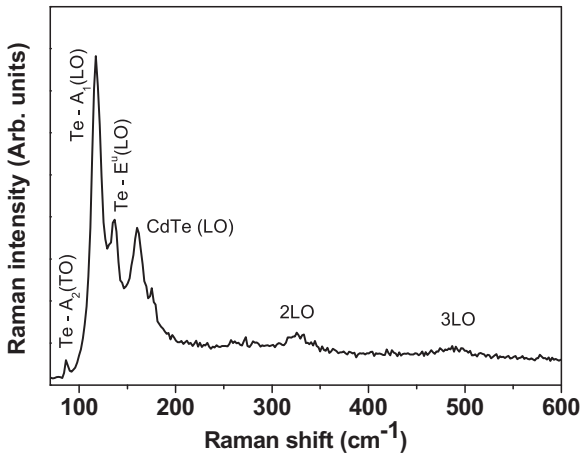

Fig. 2. Raman spectrum of the CdTe:Te thin film where the LO phonon mode plus two overtones and a Te-modes are displayed in the 170–600 cm^{-1} range.

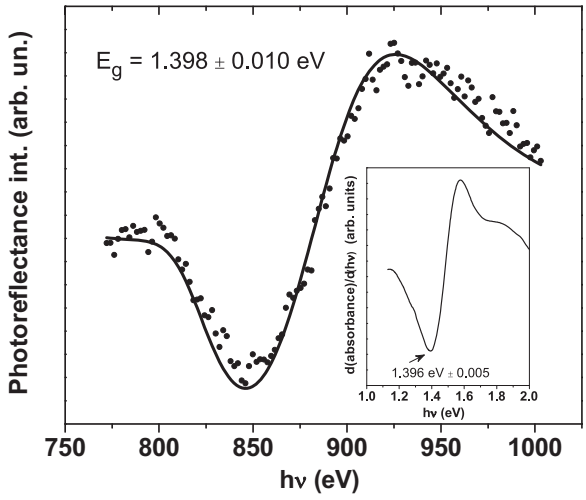

Fig. 3. Temperature modulated transmission spectrum of the CdTe:Te sample. Points represent the experimental data and the solid line the theoretical fitting to obtain the E_g value. The inset illustrates the first derivative of the optical absorption spectrum. The arrow indicates the E_g value obtained.

was in close agreement with the first derivative of the optical absorbance spectrum, see inset in Fig. 3 [16]; the values found are 1.398 ± 0.010 eV from MTS and 1.396 ± 0.006 eV from absorbance spectroscopy data. E_g = 1.40 ± 0.01 eV was taken as an acceptable band gap value for our CdTe sample. At first glance, it seems that the measured value is unusually low for CdTe semiconductor, however this behavior has been observed in semiconductors such as CdTe [17], GaAs [18], and ZnO [19] among others and it is associated to degenerated dopage [20].

The band to band PL spectrum of a CdTe:Te sample is shown in Fig. 4 at 1.4039 eV. Up to six additional signals can be observed at shorter wavelengths and two signals at larger ones. Our MTS and optical absorption measurements do not have the necessary resolution to detect that kind of electronic transitions. It is important to clarify that other similar samples with slightly different thickness and Te doping concentration do not display these type of band to band PL spectrum. In the inset of Fig. 4 the deconvolution processes followed to fit the total PL signal using Gaussian line-shape emissions is illustrated. The deconvolution fitting helps to define the maximum and the full width at half maximum (FWHM) of each line. In Fig. 5(a) the surface band bending expected for the CdTe:Te film is illustrated. The bending is

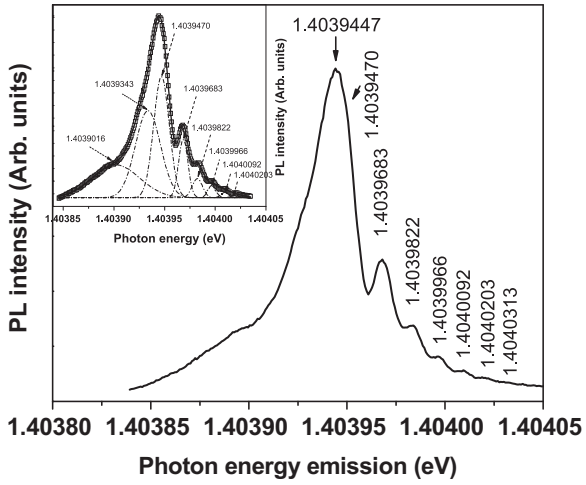

Fig. 4. The band to band photoluminescence spectrum of Fig. 4 in the photon energy range of 1.40385–1.403405 eV. The inset shows the deconvolution process carried out to define the maximum of each signal-emission.

caused by the presence of surface states [15,21–23] due to the presence of acceptor states at the CdTe:Te-air interface [23–25]. Fig. 5(b) displays a schematic representation of the built-in electric field perpendicular to surface, which in turn generates an approximated triangular potential well in the depletion region of the semiconductor [22,26,27]. In the conduction band of the depletion layer region, that, is in the triangular well potential, the states are quantized due to the confinement, where the resonantly excited 2D-electron gas confined into the region is distributed in discrete energy levels from which transitions to the valence band (VB) give place to a well defined pattern of fringes [21,28]. The pattern of recombination PL emissions follows the well known Airy pattern characteristic of a triangular well with an applied electric field [21,28,29]. The average separation between next emissions is about 12 ± 3 μeV and the FWHM of emissions is also 12 ± 3 μeV. The energy distribution of fringes can be expressed by the relationship [30,31]:

$$E_n = a + b(n-¼)^{2/3},\ n = 1, 2, \ldots$$
$$E_n = a + [(\hbar^2/2\,m^*)(3\pi q\varepsilon/2)^2]^{1/3}\{n-¼\}^{2/3},\ n = 1, 2, \ldots \quad (1)$$

where E_n is the energy of the maximum of the fringe and n is the number of the fringe, m the effective mass, q the electronic charge, $m^* = 0.11m_e$ the electron effective mass for CdTe, m_e the mass of the electron, and ε the electric field. In Fig. 6 the plot of E_n versus $(n - ¼)^{2/3}$ is displayed, in which the linear dependence of E_n versus $(n - ¼)^{2/3}$ is clearly satisfied. a = 1.4039 ± 0.0002 eV and b = 3.12 ± 0.06 eV. From the slope the calculated ε value is: 3.2 × 10^6 V/cm. The width of depletion region L is given by [30]

$$L = [(\epsilon\epsilon_0 k_B T/(q^2 p)]^{1/2} \quad (2)$$

ϵ = 10 (for CdTe), k_B the Boltzmann constant, T the absolute temperature (300 K), ϵ_0 = vacuum dielectric constant, p the holes density = 5.0 ± 0.2 × 10^{18} cm^{-3}. From Eq. (2), L = 5.35 nm, which compared with the film thickness of 250 ± 10 nm implies that the depletion region width is very close to the surface. It is worth to mention that in the absorption spectra of organic-monolayer/metal thin films slim fringes have been observed where the separation between neighbor-fringes is about 0.62 μeV and their FWHM is on the same order [32].

4. Conclusions

The high doping level attained by including additional elemental Te during the rf sputtering deposition process produces a strong surface electric field that creates a triangular well for surface carriers. The band gap value of E_g = 1.40 ± 0.01 eV measured through MTS and corroborated by absorbance spectroscopy is due to a bandgap renormalization effect because the high doping level.

The sharp fringes of the photoluminescence spectrum of a CdTe:Te thin films was fitted by means of the triangular well potential originated for the surface electric field associated to the high doping level of the CdTe sample. The PL spectrum shows an emission pattern whose theoretical approach is now part of many standard texts on quantum mechanics. The band to band electronic transitions from the discrete energy levels of the triangular well give place to an Airy pattern of fringes in the PL emission where the energy-positions are exactly predicted by the theory. The analysis allows the determination of the built-in field and the width of the depletion region.

Acknowledgements

The authors thank to M. Guerrero, A. García-Sotelo, L. Rojas and A. Soto by their technical assistance. MML Acknowledges the partial economical support to take the sabbatical leave from Departamento de Física at Centro de Investigacion y Estudios Avanzados del IPN.

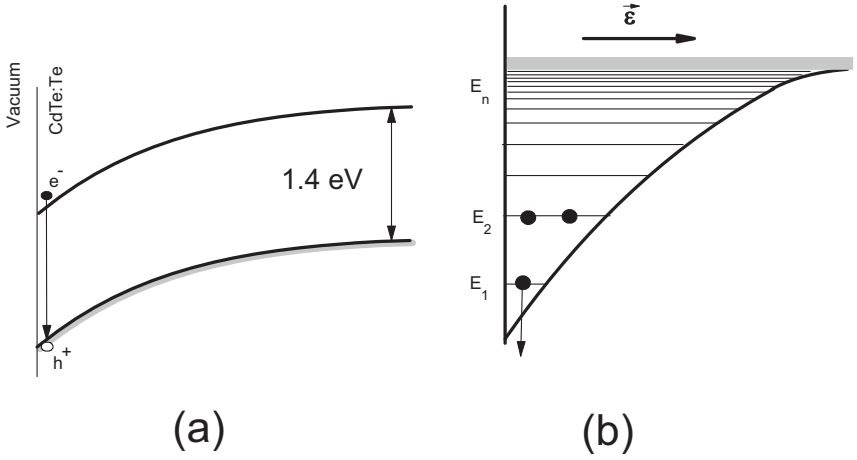

Fig. 5. (a) Schematic representation of band bending of the p-type CdTe:Te films due to the surface states at the air-CdTe:Te surface of the sample. (b) Representation of the approximated-triangular potential well with the built-in electrical field.

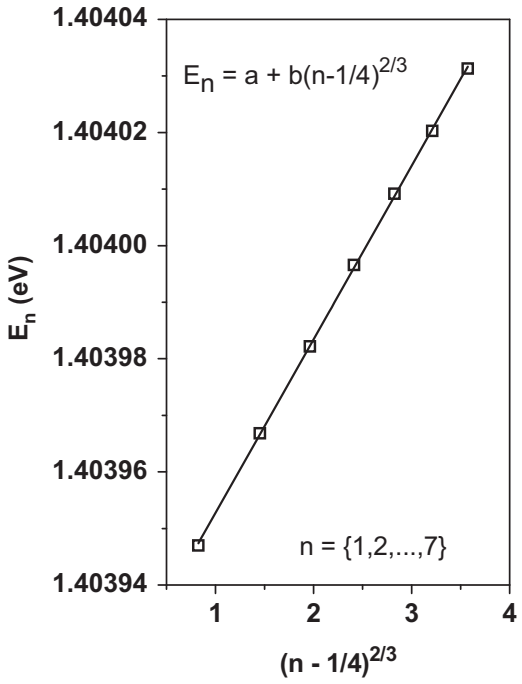

Fig. 6. Energy position E_n of each maximum of the secondary emissions of Fig. 5 against $(n - ¼)^{2/3}$. The linear fitting is clearly satisfied.

References

[1] M.O. Reese, C.L. Perkins, J.M. Burst, S. Farrell, T.M. Barnes, S.W. Johnston, D. Kuciauskas, T.A. Gessert, W.K. Metzger, Intrinsic surface passivation of CdTe, J. Appl. Phys. 118 (2015) 155305–155312.

[2] J.D. Poplawsky, Cadmium telluride solar cells: record-breaking voltages, Nat. Energy 1 (2016) 16021–16023.

[3] S. Del Sordo, L. Abbene, E. Caroli, A.M. Mancini, A. Zappettini, P. Ubertini, Progress in the development of CdTe and CdZnTe semiconductor radiation detectors for astrophysical and medical applications, Sensors 9 (2009) 3491–3526.

[4] T. Takahashi, S. Watanabe, G. Sato, Y. Okada, S. Kubo, Y. Kuroda, M. Onishis, R. Ohno, High-resolution CdTe detector and applications to imaging devices, IEEE Trans. Nucl. Sci. 48 (2001) 287–291.

[5] V. Lyahovitskaya, L. Chernyak, J. Greenberg, L. Kaplan, D. Cahen, Low temperature, post-growth self-doping of CdTe single crystals due to controlled deviation from stoichiometry, J. Appl. Phys. 88 (2000) 3976–3981.

[6] M. Cardenas, J.G. Mendoza-Alvarez, F. Sanchez-Sinencio, O. Zelaya, C. Menezes, Photoluminiscent properties of films of CdTe on glass grown by a hotwall-close space vapour transport method, J. Appl. Phys. 56 (1984) 2977–2980.

[7] J.M. Figueroa, F. Sánchez-Sinencio, J.G. Mendoza-Alvarez, O. Zelaya, C. Vázquez-López, J.S. Helman, Influence of Cd vacancies on the photoluminescence of CdTe, J. Appl. Phys. 60 (1986) 452–456.

[8] J. Aguilar-Hernández, G. Contreras-Puente, H. Flores-Llamas, H. Yee-Madeira, O. Zelaya-Angel, Photoluminescence studies of semiconducting polycrystalline CdTe films, J. Phys. D: Appl. Phys. 28 (1995) 1517–1520.

[9] O. Zelaya-Angel, M. Garcia-Rocha, J.G. Mendoza-Alvarez, M. Cardenas, J. Aguilar-Hernandez, Donor–acceptor pair photoluminescence spectra analysis in CdTe:Ag, J. Appl. Phys. 94 (2003) 2284–2288.

[10] Shen, M. Dutta, Franz–Keldysh oscillations in modulation spectroscopy, J. Appl. Phys. 78 (1995) 2151.

[11] O. Zelaya-Angel, A. Picos-Vega, R. Ramirez-Bon, F.J. Espinoza-Beltran, Interstitial Cd doping CdTe films by co-sputtering, Vacuum 52 (1999) 99–102.

[12] T.A. Gessert, S.H. Wei, J. Ma, D.S. Albin, R.G. Dhere, J.N. Duenow, D. Kuciauskas, A. Kanevce, T.M. Barnes, J.M. Burst, W.L. Rance, M.O. Reese, H.R. Moutinho, Research strategies toward improving thin-film CdTe photovoltaic devices beyond 20% conversion efficiency, Sol. Energy Mater. Sol. Cells 119 (2013) 149–155.

[13] G. Morrel, A. Reynes-Figueroa, R.S. Katiyar, M.H. Farias, F.J. Espinoza-Beltrán, O. Zelaya-Angel, F. Sánchez-Sinencio, Raman spectroscopy of oxygenated amorphous CdTe films, J. Raman Spectrosc. 25 (1994) 203–206.

[14] M. Cardona, Modulation Spectroscopy, Academic Press, N.Y., 1969.

[15] H. Shen, M. Dutta, Franz–Keldysh oscillations in modulation spectroscopy, J. Appl. Phys. 78 (1995) 2151–2155.

[16] O. Portillo-Moreno, R. Lozada-Morales, M. Rubin-Falfan, O. Zelaya-Angel, L. Baños-Lopez, Phase transformation on CdSe thin films under annealing in Ar+Se-2 atmosphere, J. Phys. Chem. Solids 61 (2000) 1751–1754.

[17] M. Kitagawa, J. Saraie, T. Tanaka, Injection electroluminescence from CdTe pn junctions prepared by LPE, Appl. Phys. A 26 (1981) 151–156.

[18] H.C. Casey Jr, F. Stern, Concentration-dependent absorption and spontaneous emission of heavily doped GaAs, J. Appl. Phys. 47 (1976) 631–643.

[19] A.P. Roth, J.B. Webb, D.F. Williams, Band-gap narrowing in heavily defect-doped ZnO, Phys. Rev. B 25 (1982) 7836–7839.

[20] A. Walsh, J.L. Da Silva, S.H. Wei, Origins of band-gap renormalization in degenerately doped semiconductors, Phys. Rev. B 78 (2008) 075211–075215.

[21] A. Chaudhry, J.N. Roy, Comparative study of energy quantization approaches in nanoscale Mosfets, J. Electron. Sci. Technol. 9 (2011) 51–57.

[22] P.A. Gentsar, A.I. Vlasenko, Investigation of electron properties of semiconductor surface by modulation spectroscopy of electroreflection, Semiconductors 40 (2006) 1066–1070.

[23] J. Misiewicz, P. Sitarek, G. Sek, R. Kudrawiec, Semiconductor heterostructures and device structures investigated by photoreflectance spectroscopy, Mater. Sci. 21 (2003) 263–318.

[24] R. Kudrawiec, M. Syperek, J. Misiewicz, M. Rudziński, A.P. Grzegorczyk, P.R. Hageman, P.K. Larsen, Below bandgap transitions in an AlGaAN/GaN transistor heterostructure observed by photoreflectance spectroscopy, Phys. Stat. Sol. C 3 (2006) 2117–2120.

[25] I. Vaquila, J.W. Rabalais, J. Wolfgang, P. Nordlander, Doping dependence of electronic charge transfer on Si(1 0 0), Surf. Sci. 489 (2001) L561–L567.

[26] Qing-An Huang, Field emission from a silicon surface potential well based on an airy function approach, J. Appl. Phys. 78 (1995) 1254–1258.

[27] D.W. Niles, X. Li, P. Sheldon, H. Höchst, A photoemission determination of the band diagram of the Te/CdTe interface, J. Appl. Phys. 77 (1995) 4489–4493.

[28] W.-H. Chang, T.M. Hsu, W.C. Lee, R.S. Chuang, A study of the Franz–Keldysh oscillations in electromodulation reflectance Si-delta-doped GaAs by a fast Fourier transformation, J. Appl. Phys. 83 (1998) 7873–7878.

[29] I.N. Yassievich, M.S. Bresler, O.B. Gusev, Yu.P. Yakovlev, Electron confinement due to reflection from the interface in heterojunctions, Phys. Status Solidi B 165 (1991) K9–K12.

[30] P.A. Gentsar, A.I. Vlasenko, A.A. Kudryatsev, Electron properties of semiconductor surface studied by the electroreflectance spectroscopy method, Semicond. Phys. Quant. Electron. Optoelectron. 8 (2005) 85–90.

[31] M.E. Flatte, M. Holthau, Classical and quantum dynamics of a periodically driven. Particle in a triangular well, Ann. Phys. 245 (1996) 113–146.

[32] M.E. Mulcahy, S.L. Berets, M. Milosevic, J. Michl, Enhanced sensitivity in single-reflection spectroscopy of organic monolayers on metal substrates (Pseudo-ATR), J. Phys. Chem. 108 (2004) 1519–1521.